ISSN 2616-5767 Vol.7, Issue 4: 114-121, DOI: 10.25236/AJETS.2024.070417

Dynamics Topology Optimization of Stiffened Plates under Time-Domain Dynamic Loads

Mingkun Guo[1,a], Zhuoyi Yang[1,b,*], Huadong Shao[1,c]

[1]Naval Architecture and Port Engineering College, Shandong Jiaotong University, Weihai, China
[a]1461189648@qq.com, [b]zhuoyi0716@126.com, [c]1725386293@qq.com
[*]Corresponding author

Abstract: *Dynamics performance is a crucial mechanical performance indicator for stiffened plates. Therefore, this paper investigates the topology optimization design for minimizing dynamic compliance of stiffened plates under time-domain loads. Based on the SIMP (Simple isotropic material with penalization), an interpolation model for stiffened plates is established. To enhance the accuracy of sensitivity calculations, a sensitivity analysis strategy that discretizes before differentiating is employed. By introducing adjoint variables, the cost of computing the gradient of the function is made linearly dependent on the number of state variables, significantly improving computational efficiency. With the constraint of the stiffener volume fraction, the topology optimization problem for minimizing dynamic compliance of stiffened plates under half-wave sinusoidal loads is solved. Finally, through a comparison of numerical results from example cases with the dynamic response of traditional unidirectional stiffened plates, it is found that the maximum displacement of the optimized stiffened plate is approximately 30.5% of the maximum displacement of the unidirectional stiffened plate. This verifies that the optimized stiffened plate exhibits superior dynamics performance.*

Keywords: *Time-domain load, Topology optimization, Dynamic compliance, Adjoint variable method*

1. Introduction

Stiffened plate structures, with their excellent specific stiffness and specific strength, are widely used in aerospace, shipbuilding, submarine, and other fields [1]. In ship structural design, stiffened plates play a crucial role in enhancing the overall rigidity and strength of the structure, significantly improving the wave-resistant performance and carrying capacity of ships. D. Quinn and A. Murphy [2] conducted research on stiffened plates in vehicles, demonstrating that the initial buckling performance can be enhanced while ensuring the lightweight of the vehicle. Xu [3] studied the ultimate strength of stiffened plates under combined transverse and longitudinal loads and derived empirical formulas to predict the collapse behavior of ship structures. Goel et al. [4] explored the dynamic response of stiffened plates under airblast loads, providing a reference for safe structural design. As an important supporting structure of submarines, the ring-stiffened cylindrical shell has also been studied by Yang et al. [5] regarding its strength and buckling performance under mechanical and thermal loads.

Stiffened plates, as a lightweight structure, have garnered widespread attention for their design methodology. Quinn et al. [6] introduced a secondary stiffener design to traditional stiffened plates and experimentally demonstrated that this secondary reinforcement design increased the initial buckling strength by 89% compared to stiffened plates of equivalent mass design. Omidali and Khedmati [7], for the first time, integrated reliability methods into the design of ship stiffened plates, taking into account the uncertainties in local load patterns caused by environmental and internal forces, thereby enhancing the safety of ship structures. Yang et al. [8] employed the nonlinear finite element method to investigate the dynamic ultimate strength of stiffened plates in the bottom of ships under uniaxial compression and lateral pressure, taking into account both material and geometric nonlinearities. Amaral et al. [9] proposed a new computational procedure for the structural design of stiffened plates with symmetric boundary conditions. This procedure always finds an appropriate geometry to transform the reference plate into stiffeners, significantly improving mechanical performance. Li et al. [10] introduced the design concept of material addition and mathematically explained the adaptive growth behavior of this branching pattern based on the Kuhn-Tucker conditions, providing a topologically optimized solution for the layout of stiffened plate/shell structures.

In the geometric optimization study of elastoplastic buckling plates with stiffeners, Lima et al. [11]

ISSN 2616-5767 Vol.7, Issue 4: 114-121, DOI: 10.25236/AJETS.2024.070417

employed a structural design approach combining exhaustive search techniques with the finite element method. They found that adjusting parameters such as the volume fraction of stiffeners, their quantity, and the ratio of stiffener height to thickness significantly affects the performance of stiffened plates under buckling. Farkas[12] improved the original Snyman-Fatti (SF) [13] global continuous optimization algorithm and applied it to the optimal design of welded square stiffened plates. By optimizing plate thickness and stiffener dimensions using a cost calculation method, while considering stress and deflection constraints, he demonstrated the effectiveness and accuracy of the SF algorithm in this structural optimization problem. Soares and Gordo [14] evaluated the performance of three designs of stiffened plates subjected to in-plane uniaxial compression loads through a comparative analysis of numerical and experimental results. They reduced deviations and uncertainties in the dataset by predicting stiffener trip phenomena. Zhao et al. [15] proposed a method combining modal superposition and model reduction techniques for the topological optimization of large structures with proportional damping under harmonic excitation. This approach effectively reduces computation time while ensuring the accuracy of optimization results. Sasikumar et al. [16] utilized topological optimization methods to explore the maximum damping capacity of passive constrained layer damping treatments, successfully identifying the optimal combination of layer thicknesses and treatment coverage areas. Similarly, Ma et al. [17] developed a generative design method and equivalent model based on the homogenization approach to optimize stiffened plates.

Despite numerous positive and significant research achievements in the field of stiffened structure design, the consideration of dynamic load scenarios is often overlooked in the critical stages of detailed design. In view of this, this paper focuses on the performance of stiffened plates under time-domain dynamic loads and innovatively proposes a dynamic topological optimization method for such complex working conditions. By combining the discretize-then-differentiate method with the adjoint method, the accuracy of sensitivity calculations is improved while reducing computational costs. Through verification with optimization design examples, the optimized stiffened plate structure significantly improves its dynamic performance under time-domain loads. The optimization scheme effectively enhances the stability of the stiffened plate when subjected to dynamic loads, with the maximum displacement in the force direction being only 30.5% of that of traditional stiffened plates. This provides a new approach for the optimal design of stiffened structures in practical engineering.

2. Topology Optimization for Minimizing Dynamic Compliance Under Volume Constraints

2.1. Material Interpolation Model

The density-based SIMP [18] method is adopted in this study, where the interpolation relationship between relative element density and element elastic modulus is

$$D_i = D_i(z_i) = D_{min} + z_i^p (D_0 - D_{min}), \quad z_i \in [0,1] \tag{1}$$

where D_0 is the material elastic modulus matrix, D_i is the interpolated element elastic modulus matrix, $D_{\min}$ is the elastic modulus of the void material, put to a small non-zero value to avoid singularity in the finite element stiffness matrix, and p is the penalty index $(p>1)$.

To address issues such as checkerboarding and local minima in topology optimization, filters are often used. The basic filtering function is defined as

$$\overline{z}_i = \frac{\sum_{j \in N_i} Q_{ij} v_j z_j}{\sum_{j \in N_i} Q_{ij} v_j} \tag{2}$$

Where N_i is the neighborhood of the element z_i with volume v_i, $j \in N_i$, Q_{ij} is the filter weight coefficient, and Q_{ij} is defined as

$$Q_{ij} = \min\{0, r_{\min} - r_{ij}\} \tag{3}$$

ISSN 2616-5767 Vol.7, Issue 4: 114-121, DOI: 10.25236/AJETS.2024.070417

Where $r_{ij} = dist(i, j)$, $r_{\min}$ is the size of the neighborhood of the unit. Replace the filter function into the SIMP interpolation model

$$D_i(\tilde{z}_i) = D_{min} + \overline{z}_i^p (D_0 - E_{min}), \ \ \overline{z}_i \in [0,1] \tag{4}$$

2.2. Formulation for Minimizing Dynamic Compliance under Volume Constraints

To solve the dynamic response problem of stiffened plates, this paper employs the finite element method as a foundation to determine the response of stiffened plates under time-domain loads. The structural motion equation under external dynamic load excitation is expressed as follows

$$M\ddot{\varsigma}_\ell + C\dot{\varsigma}_\ell + K\varsigma_\ell = f_\ell, \quad \ell = 0,\ldots,N_t \tag{5}$$

where M, C, and K are the mass, damping, and stiffness matrices, respectively, and $\ddot{\varsigma}_\ell$, $\dot{\varsigma}_\ell$, and ς_ℓ are the displacement, velocity, and acceleration vectors, respectively. N_t is the number of time steps. The mass and stiffness matrices are calculated as

$$M = \sum_{i=1}^{N} V_i \mathbf{m}_i \tag{6}$$

$$K = \sum_{i=1}^{N} E(v_i) \mathbf{k}_i \tag{7}$$

$\mathbf{m}_i$ and $\mathbf{k}_i$ are the mass matrix and stiffness matrix of the i_{th} element, respectively. In order to satisfy the finite element method, $\mathbf{m}_i$ and $\mathbf{k}_i$ are defined as follows

$$\mathbf{m}_i = \int_{\Omega_i} \rho_0 N_i^T N_i \mathrm{d}\Omega \tag{8}$$

$$\mathbf{k}_i = \int_{\Omega_i} B_i^T D_0 B_i \mathrm{d}\Omega \tag{9}$$

N and B are shape function and strain-displacement matrix, D_0 and ρ_0 are material modulus matrix and density, respectively.

To establish the relationship between the volume fraction and density of individual elements, a volume interpolation function [19] is defined based on a threshold projection function.

$$V_i = o_{\min} + (1 - o_{\min}) v_i \tag{10}$$

$$v_i = \frac{\tanh(\overline{\beta}\overline{\eta}) + \tanh\left(\overline{\beta}\left(\overline{z}_i - \overline{\eta}\right)\right)}{\tanh(\beta\overline{\eta}) + \tanh(\overline{\beta}(1 - \overline{\eta}))} \tag{11}$$

This approach allows us to accurately interpolate the volume fractions and corresponding densities across the elements. In order to prevent the numerical singularity $u_{\min}$ from being set to a positive number approaching 0, this article $o_{\min} = 0.0001$. $\overline{\beta}$ is the projection intensity, $\overline{\eta}$ is the threshold density. The material interpolation function is

$$E(v_i) = o_{\min} + (1 - o_{\min}) e(v_i) \tag{12}$$

The stiffness interpolation function based on the RAMP function is

$$e(v_i) = \frac{v_i}{1 + p\left[1 - v_i\right]} \tag{13}$$

ISSN 2616-5767 Vol.7, Issue 4: 114-121, DOI: 10.25236/AJETS.2024.070417

Where p is the RAMP punishment index. For proportional damping systems, the Rayleigh damping method is adopted to calculate the damping matrix.

$$C = \beta_r K + \alpha_r M \tag{14}$$

Where α_r and β_r are Rayleigh damping parameters.

In order to reduce the vibration of the stiffened plate under the external dynamic load, the optimization objective is to minimize the dynamic compliance of the structure and the material volume of the stiffened plate is taken as the constraint. The mathematical model is

$$\begin{aligned} &\min_{z} \ f\left(z,\varsigma_0,\ldots,\varsigma_{N_t}\right)=\frac{1}{N_t}\sum_{\ell=0}^{N_t} f_\ell^T \varsigma_\ell \\ &\text{s.t.} \ \ \mathrm{I}_j(z)=\frac{\sum_{i\in\mathcal{E}_j} J_i V_i}{\sum_{i\in\mathcal{E}_j} J_i}-\overline{v}_j \geqslant 0, \\ &M\ddot{\xi}_\ell + C\dot{\xi}_\ell + K\varsigma_\ell = f_\ell, \\ &0 \leqslant z \leqslant 1,\ 1 \leqslant j \leqslant N_j \end{aligned} \tag{15}$$

Where N_j is the number of volume limits and $\overline{v}_j$ is the specified number of volume parts.

2.3. Sensitivity Analysis

To enhance the exactness of sensitivity analysis, a "discretize-then-differentiate" strategy is employed. Using the chain rule, the relationship between the objective function f and the design variable z is expressed as

$$\frac{\mathrm{d}f}{\mathrm{d}z}=\frac{\partial f}{\partial z}+\sum_{\ell=0}^{N_t}\frac{\partial f}{\partial \varsigma_\ell}\cdot\frac{\partial \varsigma_\ell}{\partial z} \tag{16}$$

The adjoint variable method can significantly reduce the computational load during the solution process, thereby improving efficiency. Introducing three adjoint variables, $\tau_\ell, \mu_\ell, \lambda_\ell$, revise the formula (16) to

$$\frac{\mathrm{d}f}{\mathrm{d}z}=\frac{\partial f}{\partial z}+\sum_{\ell=0}^{N_t}\frac{\partial f}{\partial \zeta_\ell}\frac{\partial \zeta_\ell}{\partial z}+\sum_{\ell=1}^{N_t}\tau_\ell^{\mathrm{T}}\frac{\mathrm{d}\mathbf{R}_\ell}{\mathrm{d}z}+\sum_{\ell=1}^{N_t}\mu_\ell^{\mathrm{T}}\frac{\mathrm{d}\mathbf{P}_\ell}{\mathrm{d}z}+\sum_{\ell=1}^{N_t}\lambda_\ell^{\mathrm{T}}\frac{\mathrm{d}\mathbf{Q}_\ell}{\mathrm{d}z} \tag{17}$$

In which the initial conditions

$$\mathbf{R}_0 = M\ddot{\varsigma}_0 + C\dot{\varsigma}_0 + K\varsigma_0 - f_0 = 0 \tag{18}$$

$$\mathbf{P}_\ell = -\varsigma_\ell + \varsigma_{\ell-1} + \Delta t\,\dot{\varsigma}_{\ell-1} + \Delta t^2\left[\left(\frac{1}{2}-\beta\right)\ddot{\varsigma}_{\ell-1} + \beta\ddot{\varsigma}_\ell\right] = \mathbf{0}, \quad \ell = 1,\ldots,N_t \tag{19}$$

$$\mathbf{Q}_i = -\dot{\varsigma}_\ell + \dot{\varsigma}_{\ell-1} + \Delta t\left[(1-\gamma)\ddot{\varsigma}_{\ell-1} + \gamma\ddot{\varsigma}_\ell\right] = \mathbf{0}, \quad \ell = 1,\ldots,N_t \tag{20}$$

From (18), we know that both $\partial\mathbf{P}_\ell / \partial z$ and $\partial\mathbf{Q}_i / \partial z_e$ are 0. Assuming that the initial conditions are independent of the design variables, thus $\partial\varsigma_0 / \partial z = 0$ and $\partial\dot{\varsigma}_0 / \partial z = 0$, (17) can be rewritten in the following form

ISSN 2616-5767 Vol.7, Issue 4: 114-121, DOI: 10.25236/AJETS.2024.070417

$$\frac{\mathrm{d}f}{\mathrm{d}z}=\frac{\partial f}{\partial z}+\sum_{\ell=0}^{N_t}\tau_\ell^T\frac{\partial \mathbf{R}_\ell}{\partial z}+\left(\tau_0^T\frac{\partial \mathbf{R}_0}{\partial \ddot{\varsigma}_0}+\tau_1^T\frac{\partial \mathbf{R}_1}{\partial \ddot{\varsigma}_0}+\boldsymbol{\mu}_1^T\frac{\partial \mathbf{P}_1}{\partial \ddot{\varsigma}_0}+\lambda_1^T\frac{\partial \mathbf{Q}_1}{\partial \ddot{\varsigma}_0}\right)\cdot\frac{\partial \ddot{\varsigma}_0}{\partial z}$$
$$+\sum_{i=1}^{N_t}\sum_{\ell=1}^{N_t}\left(\tau_\ell^T\frac{\partial \mathbf{R}_i}{\partial \varsigma_\ell}+\boldsymbol{\mu}_\ell^T\frac{\partial \mathbf{P}_i}{\partial \varsigma_\ell}+\lambda_\ell^T\frac{\partial \mathbf{Q}_i}{\partial \varsigma_\ell}+\frac{\partial f}{\partial \varsigma_\ell}\right)\cdot\frac{\partial \varsigma_\ell}{\partial z}+\sum_{i=1}^{N_t}\sum_{\ell=1}^{N_t}\left(\tau_i^T\frac{\partial \mathbf{R}_i}{\partial \dot{\varsigma}_\ell}+\boldsymbol{\mu}_i^T\frac{\partial \mathbf{P}_i}{\partial \dot{\varsigma}_\ell}+\lambda_i^T\frac{\partial \mathbf{Q}_i}{\partial \dot{\varsigma}_\ell}\right)\cdot\frac{\partial \dot{\varsigma}_\ell}{\partial z}$$
$$+\sum_{i=1}^{N_t}\sum_{\ell=1}^{N_t}\left(\tau_i^T\frac{\partial \mathbf{R}_i}{\partial \ddot{\varsigma}_\ell}+\boldsymbol{\mu}_i^T\frac{\partial \mathbf{P}_i}{\partial \ddot{\varsigma}_\ell}+\lambda_i^T\frac{\partial \mathbf{Q}_i}{\partial \ddot{\varsigma}_\ell}\right)\cdot\frac{\partial \ddot{\varsigma}_\ell}{\partial z} \tag{21}$$

Finally, the sensitivity of the objective function is obtained.

$$\frac{\mathrm{d}f}{\mathrm{d}z}=\frac{\partial f}{\partial z}+\sum_{\ell=0}^{N_t}\tau_\ell^T\frac{\partial \mathbf{R}_\ell}{\partial z} \tag{22}$$

Based on the sensitivity of the topological optimization for minimizing dynamic compliance of stiffened plates mentioned above, the flowchart of the optimization process is shown in Figure1.

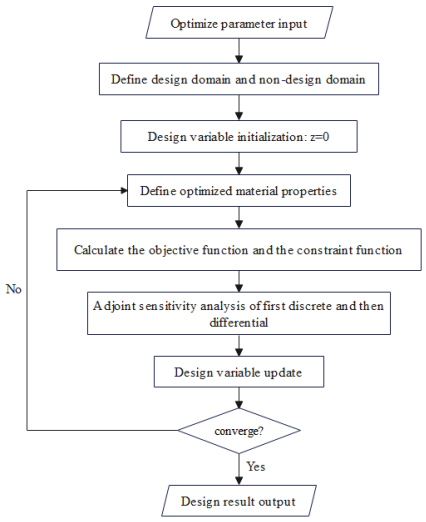

Figure 1: Topological Optimization Flowchart

3. Random Forest model training

The square plate structure with inflexible constraints on four border is selected as the optimization arrangement. As shown in figure 2, the square plate is divided into optimization region and non-optimization region in the direction of thickness, and the optimization area is divided into 19200 8-node hexahedral elements. The non-optimization area as the skin of the stiffened plate does not participate in the optimization. The center point O of the upper free surface is subjected to half-wave sinusoidal load F_t ,specific size parameters: $a=400mm$, $b=400mm$, $h=5mm$, $F_0=50N$ .The material of the stiffened plate is steel, the elastic modulus and Poisson's ratio of the material are 200Gpa and 0.3 respectively, and the mass density is 7800kg/m^3. In response to the number of sampling points $N_t=50$, solving the optimization result of minimizing the dynamic compliance of stiffened plates under the initial condition of zero, with the constraint that the volume of stiffeners does not exceed 0.15 of the optimization area volume fraction.

ISSN 2616-5767 Vol.7, Issue 4: 114-121, DOI: 10.25236/AJETS.2024.070417

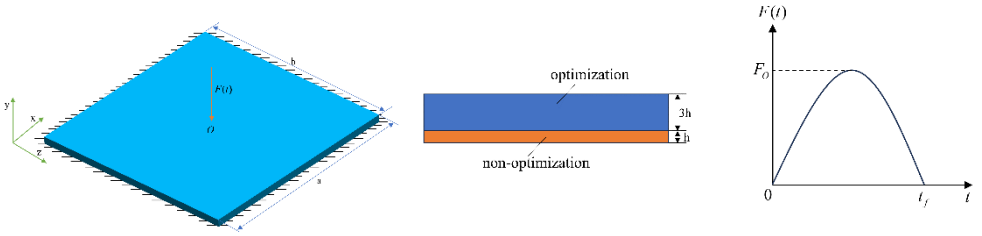

(a) Plate structure model *(b) Optimized region* *(c) Load*

Figure 2: Problem setting of stiffened plate

The iterative process and results of topology optimization of stiffened plates with four fixed edges with loading time $t_f = 0.05s$, as shown in figures 3 and 4. In the initial 20 iterations, the dynamic compliance index underwent a significant downward trajectory, indicating efficient performance improvement achieved in the early stage of structural optimization. This demonstrates the algorithm's rapid response and initial optimization capabilities for the problem. As the iterations progressed, especially after the 50th iteration, the optimization process entered a relatively stable convergence phase. Although there were occasional slight fluctuations in the objective function value during this stage, these minor changes did not substantially affect the optimization path. Instead, they reflected the high flexibility and robustness of the optimization algorithm during fine-tuning of the structural layout. This dynamic balance not only verifies the robustness of the optimization process but also ensures the reliability and accuracy of the final optimization results. The use of adjoint variables in sensitivity calculations significantly reduced the computational effort of the entire optimization process. The entire optimization was completed efficiently and accurately in just 102 iterations, achieving the expected goals.

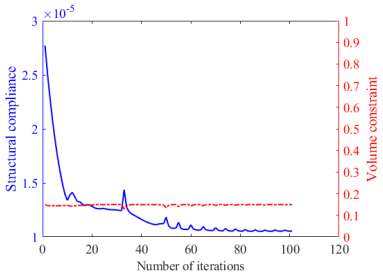

Figure 3: Iterative process

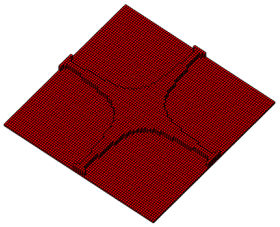

Figure 4: Optimization result

The optimization results shown in Figure 4 reveal that the distribution of stiffeners takes on a "+" shape. Since the semi-sinusoidal time-domain dynamic load is concentrated at the center of the stiffened plate, most of the stiffeners are concentrated in the middle of the plate to reduce the vibration caused by dynamic forces on the plate structure. Moreover, the intersections of the stiffeners are smoothly transitioned, which can prevent stress concentration, aligning with practical engineering design principles.

Figure 5 shows a common unidirectional stiffened panel, whose skin dimensions and stiffener volume are the same as those of the optimized stiffened panel. Dynamic analysis is conducted on this panel after subjecting to the same time-domain loads and constraints as the optimized stiffened panel.

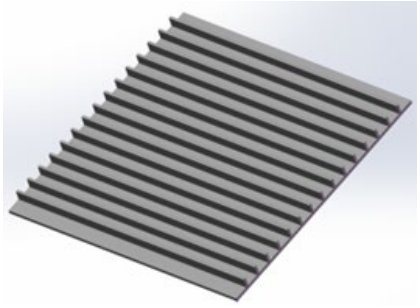

Figure 5: Unidirectional stiffened panel

The time-domain dynamic responses at the load application points of the optimized stiffened panel and the common unidirectional stiffened panel are shown in Figures 6 and 7. From Figures 6 and 7, it is

ISSN 2616-5767 Vol.7, Issue 4: 114-121, DOI: 10.25236/AJETS.2024.070417

evident that the displacement response, velocity response, and acceleration response of the topologically optimized stiffened panel under time-domain dynamic loading are significantly smaller than those of the unidirectional stiffened panel. Compared to the unidirectional stiffened panel, the maximum displacement of the optimized stiffened panel is reduced by 69.5%, the maximum velocity is reduced by 63.6%, and the maximum acceleration is reduced by 68.5%. This indicates that the stiffened panel designed in this paper demonstrates superior dynamic performance and more significant vibration reduction effects compared to common unidirectional stiffened panels when subjected to time-domain dynamic loads.

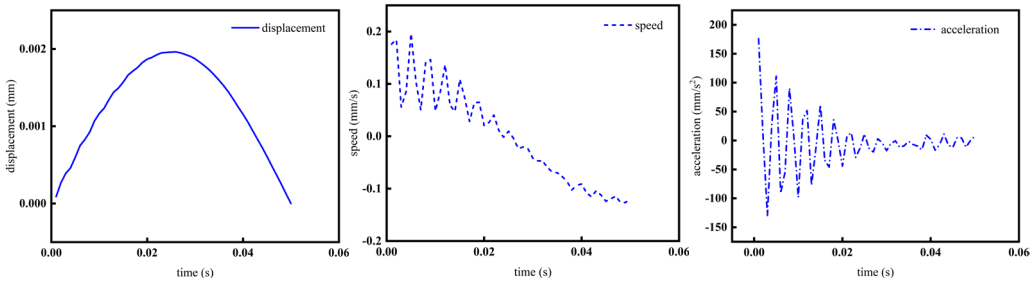

(a) Displacement *(b) Velocity* *(c) Acceleration*

Figure 6: Dynamic response of the optimized stiffened panel

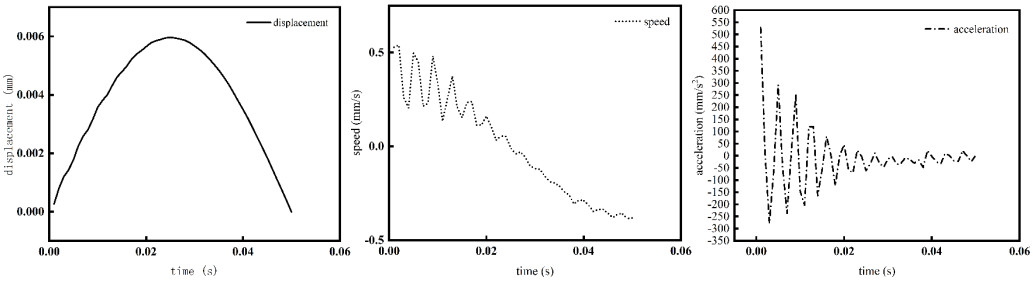

(a) Displacement *(b) Velocity* *(c) Acceleration*

Figure 7: Dynamic response of the unidirectional stiffened panel

4. Conclusion

In this study, an efficient optimization design algorithm for stiffened panels under time-domain loads is proposed, aiming to design the stiffener distribution that minimizes the dynamic compliance of the stiffened panels. We hope that the optimized stiffened panels will have better vibration reduction effects. By comparing the optimized example of a four-edge fixed stiffened panel with a regular stiffened panel, we can draw the following conclusions:

(1) Employing a sensitivity analysis strategy that involves discretization followed by differentiation, combined with the adjoint variable method, can significantly reduce computation time and enhance optimization efficiency. This strategy enables the rapid derivation of optimization results with fewer iteration steps, thereby greatly improving the convenience and practicality of computations.

(2) Under time-domain loads, the stiffened panel designed in this paper demonstrates significantly reduced vibration response in the direction of force application compared to common unidirectional stiffened panels, exhibiting superior dynamic performance.

(3) The optimized stiffened panel designed in this paper features rounded corners for smooth transitions at the intersections of stiffeners in different directions. This not only enhances the vibration reduction effect of the stiffened structure but also effectively reduces local stress concentration. This innovative design is more suitable for practical engineering applications and provides a certain guiding significance.

References

[1] Bedair O. Analysis and limit state design of stiffened plates and shells: a world view [J]. Applied Mechanics Reviews, 2009, 62(2):020-801.

ISSN 2616-5767 Vol.7, Issue 4: 114-121, DOI: 10.25236/AJETS.2024.070417

[2] Quinn D, Murphy A, McEwan W, et al. Non-prismatic sub-stiffening for stiffened panel plates—Stability behaviour and performance gains[J]. Thin-Walled Structures, 2010, 48(6): 401-413.
[3] Xu M C, Song Z J, Zhang B W, et al. Empirical formula for predicting ultimate strength of stiffened panel of ship structure under combined longitudinal compression and lateral loads [J]. Ocean Engineering, 2018, 162: 161-175.
[4] Goel M D, Matsagar V A, Gupta A K. Dynamic response of stiffened plates under air blast[J]. International Journal of Protective Structures, 2011, 2(1): 139-155.
[5] Yang Y, Li J J, Zhang Y, et al. A semi-analytical analysis of strength and critical buckling behavior of underwater ring-stiffened cylindrical shells[J]. Engineering Structures, 2021, 227: 111396.
[6] Quinn D, Murphy A, McEwan W, et al. Stiffened panel stability behaviour and performance gains with plate prismatic sub-stiffening[J]. Thin-Walled Structures, 2009, 47(12): 1457-1468.
[7] Omidali M, Khedmati M R. Reliability-based design of stiffened plates in ship structures subject to wheel patch loading[J]. Thin-Walled Structures, 2018, 127: 416-424.
[8] Yang B, Wu J, Soares C G, et al. Dynamic ultimate strength of outer bottom stiffened plates under in-plane compression and lateral pressure[J]. Ocean Engineering, 2018, 157: 44-53.
[9] Amaral R R, Troina G S, Fragassa C, et al. Constructal design method dealing with stiffened plates and symmetry boundaries[J]. Theoretical and Applied Mechanics Letters, 2020, 10(5): 366-376.
[10] Li B, Hong J, Wang Z, et al. An innovative layout design methodology for stiffened plate/shell structures by material increasing criterion[J]. Journal of engineering materials and technology, 2013, 135(2): 021012.
[11] Lima J P S, Cunha M L, dos Santos E D, et al. Constructal Design for the ultimate buckling stress improvement of stiffened plates submitted to uniaxial compressive load[J]. Engineering Structures, 2020, 203: 109883.
[12] Farkas J, Jármai K, Snyman J A. Global minimum cost design of a welded square stiffened plate supported at four corners[J]. Structural and Multidisciplinary Optimization, 2010, 40: 477-489.
[13] Snyman J A, Fatti L P. A multi-start global minimization algorithm with dynamic search trajectories [J]. Journal of optimization theory and applications, 1987, 54: 121-141.
[14] Soares C G, Gordo J M. Design methods for stiffened plates under predominantly uniaxial compression [J]. Marine Structures, 1997, 10(6): 465-497.
[15] Zhao X, Wu B, Li Z, et al. A method for topology optimization of structures under harmonic excitations [J]. Structural and Multidisciplinary Optimization, 2018, 58: 475-487.
[16] Sasikumar K S K, Arulshri K P, Selvakumar S. Optimization of constrained layer damping parameters in beam using taguchi method[J]. Iranian Journal of Science and Technology, Transactions of Mechanical Engineering, 2017, 41: 243-250.
[17] Ma X, Wang F, Aage N, et al. Generative design of stiffened plates based on homogenization method[J]. Structural and Multidisciplinary Optimization, 2021, 64: 3951-3969.
[18] Zhou M, Rozvany G I N. The COC algorithm, Part II: Topological, geometrical and generalized shape optimization [J]. Computer methods in applied mechanics and engineering, 1991, 89(1-3): 309-336.
[19] Wang F, Lazarov B S, Sigmund O. On projection methods, convergence and robust formulations in topology optimization [J]. Structural and multidisciplinary optimization, 2011, 43: 767-784.